

The Microstructure of Polyacrylonitrile-Stabilized Fibers

Heyi Ge,¹ Huashi Liu,¹ Juan Chen,¹ Chengguo Wang²

¹School of Material Science and Engineering, University of Jinan, Jinan 250022, China

²School of Material Science and Engineering, Shandong University, Jinan 250061, China

Received 30 October 2008; accepted 14 March 2009

DOI 10.1002/app.30416

Published online 27 April 2009 in Wiley InterScience (www.interscience.wiley.com).

ABSTRACT: The microstructure of the polyacrylonitrile (PAN)-stabilized fibers was investigated by X-ray diffraction (XRD), scanning electron microscope (SEM), transmission electron microscope (TEM), and high-resolution transmission electron microscope (HRTEM). XRD analysis indicated that the chemical reactions sped up notably when temperature was above 250°C. The crosssection SEM image of the stabilized fibers presented concentric multi-layer morphology. TEM images showed that the lamellar-like skin was compact and the core was disorderly and loose. The vermiculate-like crystallites in the precursor

fibers were transferred to spheres during stabilization process. HRTEM images showed that many spheres existed in the stabilized fibers. The exterior of spheres which had annular structure was amorphous phase. The inner of spheres which was not completely stabilized had some crystallite areas. © 2009 Wiley Periodicals, Inc. *J Appl Polym Sci* 113: 2413–2417, 2009

Key words: PAN-stabilized fibers; crystallite; skin-core structure; spheres

INTRODUCTION

Nowadays, polyacrylonitrile (PAN)-based carbon fibers are becoming the key materials in aviation and composites owing to their high performance. It has been widely convinced that the properties of carbon fibers are mainly determined by the microstructure of precursor fibers and stabilized fibers because of the structural inheritance.^{1–3} PAN precursor fibers is rapidly heated to about 300°C in an oxidizing atmosphere to maintain good high temperature properties and to increase the yield of solid material.⁴ The stabilized fibers have been the subject of much study because it is costly and involves a number of chemical reactions.^{4–7} Therefore, study on the microstructure of PAN-stabilized fibers is pretty important to facilitate the improvement of carbon fiber properties.

Some literatures have reported the structure of PAN-stabilized fibers.^{4–9} Warner et al.⁴ examined the crosssection of stabilized fibers, which displayed a two-zone morphology, the dark-colored exterior zone and the cream-colored interior. Ko et al.⁵ investigated the morphology and microstructure of a stabilized fiber, nonburning fiber under optical and electron microscopes. Skin-core morphology was

found in the crosssection of the stabilized fiber. The model of the stabilized fiber was consistent with the lamellar plate-like structure. Various reaction schemes have been proposed to occur during stabilization, as reviewed by Bashir.⁶ It is generally thought that the good degree of molecular orientation in the PAN precursor fiber is propitious to the mechanical properties of the resultant carbon fiber.^{7–9} However, despite many years of research, there is still much uncertainty regarding the nature of the molecular order and the microstructural and chemical changes, which take place during stabilization.

There are few studies on revealing the microstructure of stabilized fibers by TEM and HRTEM because it is difficult to obtain some useful and integrated images. The aim of this study was to investigate and analyze the microstructure of stabilized fibers in detail. Thus the ion-plasma etched stabilized fiber samples and ultrathin sections of stabilized fiber samples were studied using TEM and HRTEM, respectively. It would be informative to probe into the evolution from PAN precursor fiber to stabilized fiber during stabilization. Analyses by XRD and SEM were also carried out in this study.

EXPERIMENTAL

Preparation of PAN precursor fibers

Acrylonitrile (AN) and itaconic acid (IA) were copolymerized in dimethylsulphoxide with azobisisobutyronitrile (AIBN) as radical initiator. The total concentration of monomers was controlled at 20 wt %. The ratio of AN/IA/AIBN is 98/2/0.8 (w/w/w). The

Correspondence to: H. Ge (mse_gehy@ujn.edu.cn).

Contract grant sponsor: Shandong Encouraging Fund of Excellent Scientists; contract grant number: 2008BS04035.

Contract grant sponsor: Doctoral Fund of University of Jinan; contract grant number: XBS0812.

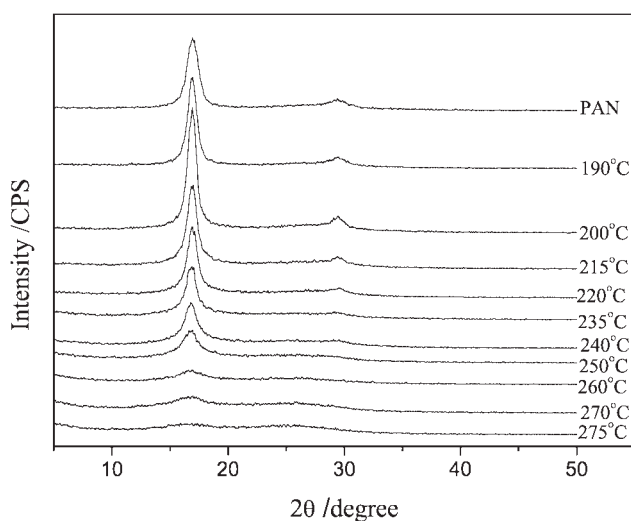


Figure 1 XRD patterns of PAN precursor fibers and the fibers stabilized at various stages.

molecular weight (M_n) of the copolymer calculated from Mark-Houwink equation was 141,000. The dope was extruded under pressure through a 1000-hole spinneret with 0.06-mm hole diameter and passed through three coagulation baths to get gel fibers. Next, the gel fibers were adequately washed with water and were drawn through three drawing processes including hot-water drawing, boiling-water drawing, and high-pressure steam drawing. Then, the filaments were finished, dried, and heat setting into the precursor fibers.

Stabilization

Two horizontal stabilization furnaces were used for stabilization. The length of each stabilization zone was 3 m and had some separated temperature zones. The temperature zones of the two stabilization furnace were from 190 to 275°C. The precursor fibers were thermal stabilized in air atmosphere under a 5% stretching ratio. The stabilization time in each stabilization zone was 6 min. The total stabilization time was about 60 min.

Characterization

A Rigaku D/max-RC diffractometer with Ni-filtered $\text{CuK}\alpha$ radiation ($\lambda = 1.5418 \text{ \AA}$) was utilized to obtain XRD patterns of PAN-stabilized fibers at various stages. The crystallite size of the laterally order domains (L_c) was estimated by Scherrer equation:

$^{10}L_c = \frac{K\lambda}{B \cos \theta}$, where λ is the wavelength of $\text{CuK}\alpha$ X-ray, B is the full width at half maximum intensity of the peak around $2\theta = 17^\circ$, and K is a constant 0.89. Aromatic Index: $\text{AI} = \frac{I_A}{I_A + I_P}$, where I_A is the intensity of the diffraction peak at around $2\theta = 25.5^\circ$, and I_P is the intensity of the diffraction peak at around $2\theta = 17^\circ$. A tow of 1000 single fibers was cut and embedded straightly in E-44 epoxy resin. After solidification, the sample was polished and then observed under HITACHI S-2500 (Japan) SEM (operated at 20 kV). The microstructure of fibers was studied by a HITACHI H-800 (Japan) TEM operated at 150 kV. Before observation, the fibers were ion-plasma etched in oxygen for 10–60 min. Moreover, a Tecnai 20 II-Twin HRTEM (operated at 200 kV) was used. The fibers were embedded in an epoxy resin. Transverse sections and longitudinal sections thinner than 30 nm were cut on a Reichert-Jung ultramicrotome with a diamond knife and collected on Formvar-coated 400-mesh copper grids.

RESULTS AND DISCUSSION

XRD investigation

The XRD patterns of PAN precursor fibers and the fibers stabilized at various stages are shown in Figure 1. The strongest diffraction peak of PAN precursor fibers occurs at around $2\theta = 17^\circ$, which corresponds to a planar spacing $d = 5.240 \text{ \AA}$ indexed to the (100) plane of a hexagonal structure.¹¹ The intensity at about $2\theta = 17^\circ$ increases gradually below 200°C and then reduces gradually above 215°C. The crystallite size (L_c) could be easily calculated via Scherrer equation, as listed in Table I. It indicates that the crystallite size first increased at the beginning of stabilization, and then decreased when the temperature rose to above 240°C. This suggested that the molecular chains around crystallites rearranged because of molecular heat motion. In initial stabilization stages, it was propitious to the increase of crystallite size. Subsequently, a new wide diffraction peak at about $2\theta = 25.5^\circ$ appears (Fig. 1), signifying that the ladder polymer structure had been transferred from the PAN structure. It increases gradually with the rise of temperature, which suggested that when it reached the crystal transition temperature, oxidation reaction and cyclization reaction in crystallite areas became intense and the crystallite structure began to change gradually above 240°C.

TABLE I
The Relationship of Aromatic Index (AI) and Temperature

| Temperature (°C) | PAN precursor fibers | 190 | 200 | 215 | 220 | 235 | 240 | 250 | 260 | 270 | 275 |
|-----------------------|----------------------|--------|--------|--------|--------|--------|--------|--------|-------|-------|-------|
| Crystallite size (nm) | 8.436 | 11.824 | 12.315 | 12.436 | 12.550 | 12.708 | 12.862 | 12.014 | 8.826 | 6.575 | 5.043 |
| AI | – | – | – | – | – | – | 0.10 | 0.16 | 0.28 | 0.42 | 0.52 |

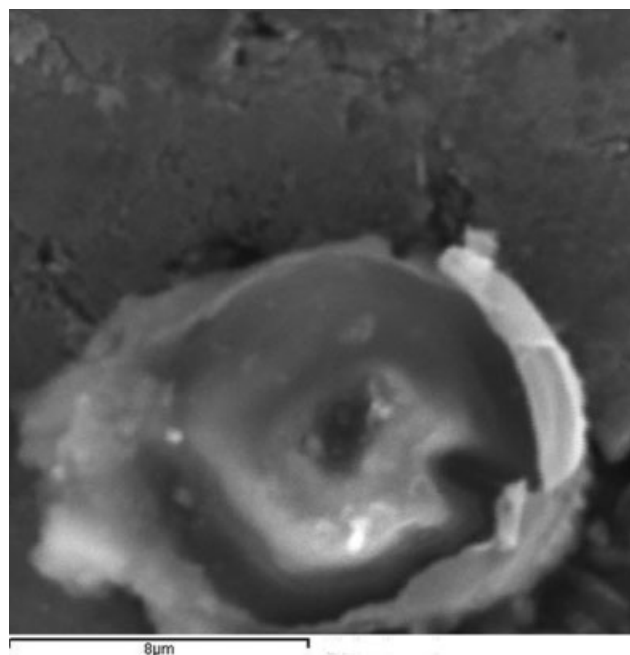


Figure 2 The crosssection of PAN-stabilized fiber.

The XRD patterns were handled via Origin 7.0 software to analyze AI tabulated in Table I. From Table I, AI rises pretty fast above 250°C, which indicates that the transformation of the microstructure in fibers speeds up. At the end of stabilization process, AI reaches 0.52 and the fibers have changed thoroughly into another new structure.¹² Thus, once temperature exceeds 250°C, it has notable influence on the stabilization degree of PAN fibers.

SEM investigation

Figure 2 is the cross-sectional SEM image of the stabilized fiber. It can be clearly seen that in the cross-section, there is not only the skin-core morphology

but also a concentric multilayer structure. The white outmost layer is the thin and dense skin, followed by the cortex layer, the endothelium layer, and the core. The interfaces among the four layers are not clear. The diameter of the stabilized fibers is about 10–11 μm. From the skin to the core, the thickness of each layer is about 0.5, 1.5, 2.5, and 2.0 μm, respectively. This structure of the stabilized fibers evolves from that of PAN precursor fibers¹³ through stabilization process.

TEM investigation

Figure 3(a) displays a typical microstructure of the stabilized fibers. The stacked sheets of the skin are compact and almost perpendicular to the fiber axis. However, in the core, the lamellar-like texture becomes loose, somewhat disorderly and unsystematic. This indicates that the perfection and orientation of texture structure decreases from the skin to the core. It is assumed that the structure is composed of planar structure, which is formed due to the cyclization of nitrile groups.¹⁴ The low oxygen content is one of the reasons of the loose microstructure in the core because the oxygen reaction can facilitate the formation of the compact structure such as the aromatic structure and cross-linking structure.^{15,16}

The skin of a filament and its magnified image are illustrated in Figure 3(b) and (c), respectively. There are some black particulates in the microstructure of the skin. Compared with that of PAN precursor fibers [Fig. 3(d)], the vermiculate-like crystallites in the precursor fibers were transferred to global particulates due to complicated reactions during stabilization process. This will be further discussed in HRTEM investigation.

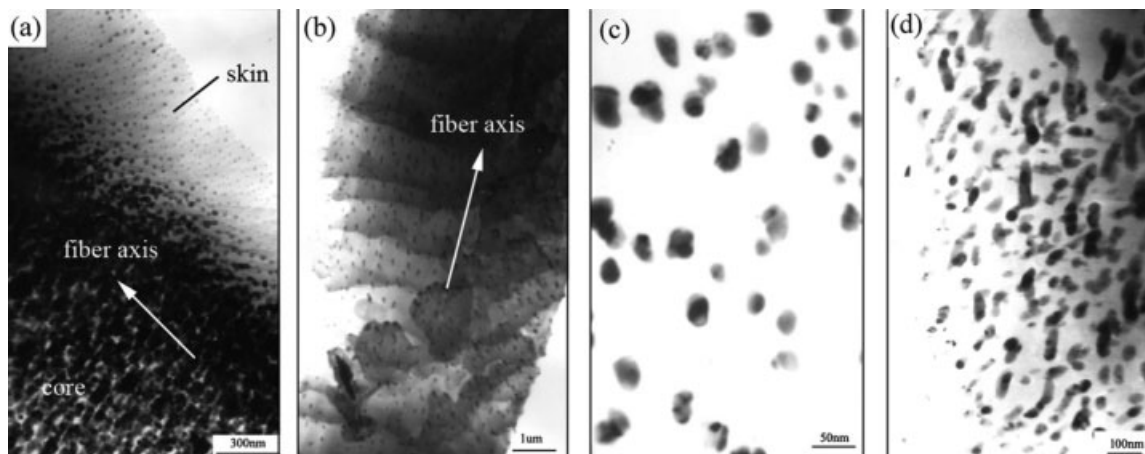


Figure 3 TEM images of PAN-stabilized fibers and PAN precursor fibers. (a) the typical microstructure of PAN-stabilized fibers, (b) the skin texture of PAN-stabilized fibers, (c) the magnified skin texture image of PAN-stabilized fibers, (d) the skin texture of PAN precursor fibers.

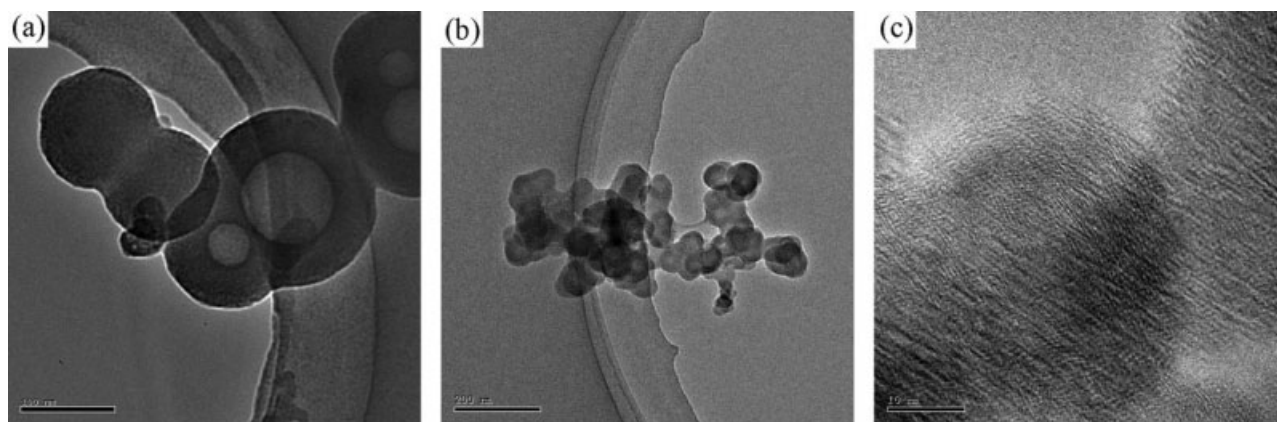


Figure 4 HRTEM images of the transverse section of PAN precursor fibers and stabilized fibers. (a) Spheres of PAN precursor fibers, (b) spheres of PAN-stabilized fibers, and (c) the magnified sphere image of PAN-stabilized fibers.

HRTEM investigation

Figure 4 is the HRTEM images obtained from the transverse section of PAN precursor fibers and stabilized fibers. Figure 4(a) represents one of the typical low magnification microstructure of PAN precursor fibers. Many spheres that interlink each other can be clearly observed. The larger spheres usually contain some smaller ones. The diameter of the spheres ranges from 10 to 100 nm. Other researchers¹⁷ observed the similar spheres in PAN precursor fibers. The spheres have actually onion-like fullerene structures including a lot of curved and concentric segments. Although the formation mechanism of these onion-like spheres in PAN fibers is presently unclear, a preliminary interpretation for it can be proposed in terms of dipolar nitrile group interactions.¹⁷

Analogous global structure can also be found in HRTEM image of the transverse section of PAN-stabilized fibers, as shown in Figure 4(b). The diameter of the spheres has decreased to about 20–30 nm. Obviously, the spheres of the stabilized fibers are transformed from that of PAN precursor fibers. The decrease of size is due to the thorough oxidization reactions and cyclization reactions in the exterior of spheres, as shown in Figure 4(c). The exterior of spheres is lamellar-like amorphous texture, annularly encircling the center. However, nanosized crystallites are seen existing in the interior of spheres. The size of the crystallites accords with the calculation via XRD analysis (Table I). Some clear crystallite structures, which are analogous to those observed in carbon fibers by HRTEM, have various orientations in different crystallites. This microstructure indicates that in stabilization process the oxidization reactions and cyclization reactions of spheres diffuse from the surface to the core. If the size of spheres is too large, it will lead to inadequate stabilized reactions in the core. Appropriate size of spheres will be propitious

to the degree of stabilization. Thus, the size and uniformity of spheres in PAN precursor fibers will directly influence the microstructure of stabilized fibers and the degree of stabilization. To manufacture high-performance carbon fibers, it is a key factor to make spheres smaller and improve their uniformity.

The microstructure of interlaced amorphous texture and crystalloid texture can also be found in the longitudinal sections of PAN-stabilized fibers, as shown in Figure 5. The spheres distribute in the amorphous texture. Likewise, many nanosized crystallites having different orientations spread around the spheres. The formation of the microstructure might be consanguineously interrelated with the orientations of PAN molecule chains in precursor fibers. The stripe structure in the underside of the

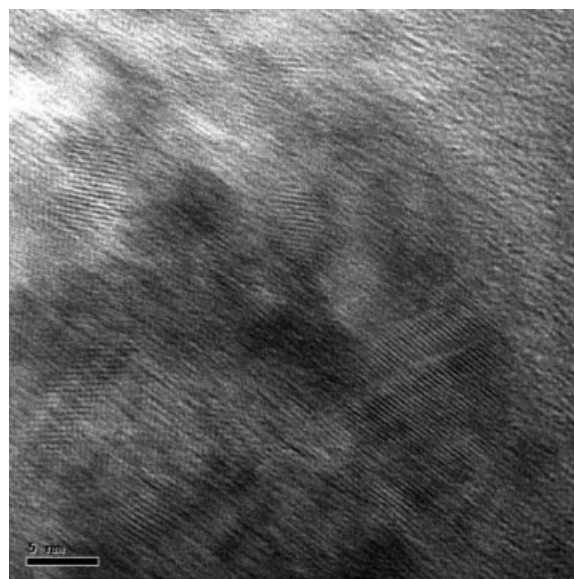


Figure 5 HRTEM image of the longitudinal section of the stabilized PAN fibers.

right (Fig. 5) is composed of two parts. The upper part is crystallite structure due to unthoroughly stabilized PAN molecule chains. The underside part is amorphous texture remaining the orientation evolved from stabilized PAN molecule chains. Therefore, the orientation and arrangement of PAN molecule chains in precursor fibers will directly influence that of molecule chains in stabilized fibers.

CONCLUSIONS

By systematic examination on the microstructure of PAN-stabilized fibers, using XRD, SEM, TEM, and HRTEM, significant structural information has been achieved. When temperature preponderated over 250°C, the transformation of the microstructure in fibers sped up notably. It might have greater influence on the stabilization degree of PAN fibers. PAN-stabilized fibers had remarkable skin-core structure. The lamellar-like skin was compact and homogeneous. However, the core was loose and somewhat disorderly. The formation of the skin-core morphology has been caused by oxygen diffusion motion and the evolution of PAN precursor fiber structure. Meanwhile, the vermiculate-like crystallites in the precursor fibers were transferred to spheres during stabilization process. In PAN-stabilized fibers, there were many nanosized spheres, which had nucleus-shell microstructure. The exterior of the

spheres was lamellar-like amorphous texture, annularly encircling the center. However, crystallites were seen existing in the interior of the spheres. From these investigations, it can be concluded that controlling the size of crystallites and the orientation of PAN molecule chains in precursor fibers will directly influence those in stabilized fibers.

References

1. Kobets, L. P.; Deev, I. S. *Comp Sci Technol* 1997, 57, 1571.
2. Chen, J. C.; Harrison, I. R. *Carbon* 2002, 40, 25.
3. Zhang, W. X.; Liu, J.; Wu, G. *Carbon* 2003, 41, 2805.
4. Warner, S. B.; Peebles, L. H., Jr.; Uhlmann, D. R. *J Mater Sci* 1979, 14, 556.
5. Ko, T. H.; Ting, H. Y.; Lin, C. H. *J Appl Polym Sci* 1988, 35, 631.
6. Bashir, Z. *Carbon* 1991, 29, 1081.
7. Bahl, O. P.; Mathur, R. B.; Kundra, K. D. *Fibre Sci Tech* 1981, 15, 147.
8. Chari, S. S.; Bahl, O. P.; Mather, R. B. *Fibre Sci Tech* 1981, 15, 153.
9. Ogawa, H.; Saito, K. *Carbon* 1995, 33, 783.
10. Gupta, V. B.; Kumar, S. *J Appl Polym Sci* 1981, 26, 1865.
11. Ko, T. H.; Lin, C. H.; Ting, H. Y. *J Appl Polym Sci* 1989, 37, 553.
12. Mathur, R. B.; Bahl, O. P.; Mittal, J.; Nagpal, K. C. *Carbon* 1991, 29, 1059.
13. Ge, H. Y.; Liu, H. S.; Chen, J. *J Appl Polym Sci* 2008, 108, 947.
14. Zhao, L. R.; Jang, B. Z. *J Mater Sci* 1997, 11, 2811.
15. Jain, M. K.; Abhiraman, A. S. *J Mater Sci* 1987, 22, 278.
16. Clarke, A. J.; Bailey, J. E. *Nature* 1973, 243, 146.
17. Bai, Y. J.; Wang, C. G.; Lun, N. *Carbon* 2006, 44, 1773.